Food & Function

Accepted Manuscript

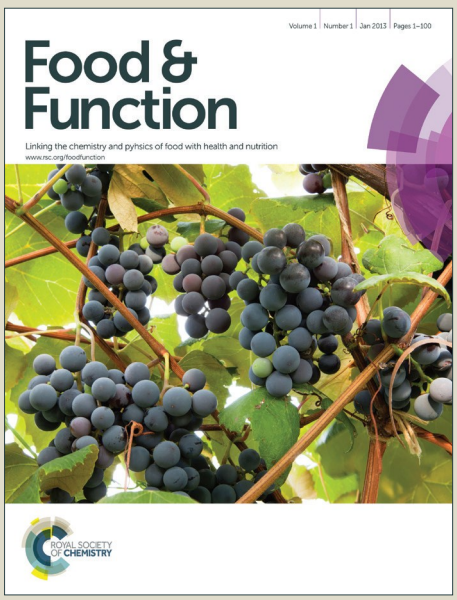

This is an *Accepted Manuscript*, which has been through the Royal Society of Chemistry peer review process and has been accepted for publication.

Accepted Manuscripts are published online shortly after acceptance, before technical editing, formatting and proof reading. Using this free service, authors can make their results available to the community, in citable form, before we publish the edited article. We will replace this *Accepted Manuscript* with the edited and formatted *Advance Article* as soon as it is available.

You can find more information about *Accepted Manuscripts* in the Information for Authors.

Please note that technical editing may introduce minor changes to the text and/or graphics, which may alter content. The journal's standard Terms & Conditions and the Ethical guidelines still apply. In no event shall the Royal Society of Chemistry be held responsible for any errors or omissions in this *Accepted Manuscript* or any consequences arising from the use of any information it contains.

ROYAL SOCIETY OF CHEMISTRY

www.rsc.org/foodfunction

Isolation and antitumor efficacy evaluation of a polysaccharide from *Nostoc commune* Vauch.

Min Guo[a,1], Guo-Bin Ding[a,1], Songjia Guo[a], Zhuoyu Li[a,b,*], Liangqi Zhao[a], Ke Li[c], Xiangrong Guo[d]

[a] Institute of Biotechnology, the Key Laboratory of Chemical Biology and Molecular Engineering of Ministry of Education, Shanxi University, Taiyuan 030006, People's Republic of China

[b] College of Life Science, Zhejiang Chinese Medical University, Hangzhou 310053, People's Republic of China

[c] Modern Research Center for Traditional Chinese Medicine, Shanxi University, Taiyuan 030006, People's Republic of China

[d] Clinical Laboratory, Shanxi Coal Center Hospital, Taiyuan 030006, People's Republic of China

[1] Both these authors contributed equally to this work.

Corresponding author: Prof. Zhuoyu Li

E-mail addresses: lzy@sxu.edu.cn.

Tel.: +86-351-7018268; Fax: +86-351-7018268.

Food & Function Accepted Manuscript

ABSTRACT

Nostoc commune Vauch. has been traditionally used as a healthy food and medicine for centuries especially in China. It has been demonstrated that the polysaccharides isolated from *Nostoc commune* Vauch. exhibit strong antimicrobial and antioxidant activities. However, little is known about their anticancer property and the underlying mechanisms of action. Herein, we report the isolation of a polysaccharide from *Nostoc commune* Vauch. (NVPS), and its physicochemical properties were analyzed. In an attempt to demonstrate the potential application of NVPS in tumor chemotherapy, the *in vitro* antitumor activity was determined. NVPS significantly suppressed the growth and proliferation of MCF-7 and DLD1 cells. The molecular mechanism underlying this *in vitro* antitumor efficacy was elucidated, and the results indicated that NVPS simultaneously triggered intrinsic, extrinsic and endoplasmic reticulum stress (ERS)-mediated apoptotic signaling pathways. Collectively, these findings demonstrate that NVPS could be used as a novel promising source of natural antitumor agent.

Keywords: *Nostoc commune* Vauch., polysaccharide, NVPS, antitumor efficacy, apoptosis

1. Introduction

The cyanobacterium *Nostoc commune* Vauch., popularly named *Nostoc commune*, belongs to the colonial form of Nostoc.[1] It distributes widely around the world, especially in China.[2] Colonies of *Nostoc commune* Vauch., harvested from natural localities, have been highly appreciated by consumers for centuries in China

Food & Function Accepted Manuscript

and increasingly recognized by people in other countries.[3] It has been claimed that the edible terrestrial alga has high nutritional value, because it contains abundant protein[4-7]and dietary fiber,[6] carbohydrates, a great variety of vitamins and mineral elements, lower fat,[7-8] and other nutrients. Indeed, *Nostoc commune* Vauch. has been shown to exhibit a broad spectrum of biological activities, such as antitumor,[9] antimicrobial,[10,11] anti-inflammation and antioxidant[12,13] properties. In our previous study, we purified and identified a water stress protein (WSP1) from *Nostoc commune* Vauch., and evaluated its antitumor effects both *in vitro* and *in vivo*.[9]

Cancer still remains one of the most deadly diseases and a global threat to human health and life. Taking into account the serious side effects and toxicity of conventional chemotherapeutic agents,[14,15] a great deal of research effort has been focused on discovering anticancer polysaccharides or complexes from natural resources for the development of effective and safe therapeutics. Commonly known as a structurally diverse class of biomacromolecules, polysaccharides play diverse and crucial roles in many biological processes.[16] In recent years, polysaccharides derived from natural resources have attracted considerable attention due to their non-toxicity even at higher concentration, higher efficiency and potential therapeutic applications.[17,18] It has been documented that polysaccharides isolated from *Nostoc commune* Vauch. exhibit a range of biological activities, including antimicrobial and antioxidant effects.[19-21] However, to the best of our knowledge, there have been few studies into the anticancer efficacy of polysaccharides from *Nostoc commune* Vauch..

In the present investigation, we isolated a polysaccharide from *Nostoc commune*

Food & Function Accepted Manuscript

Vauch. (NVPS) and examined its antitumor activity for the first time. The molecular weight of NVPS was about 2.4×10^5 Da as determined by high-performance gel permeation chromatography (HPGPC). The cell viability, apoptosis, and changes in the protein levels involved in intrinsic and extrinsic apoptotic signaling pathways after NVPS exposure were assessed. Moreover, quantitative real-time PCR and western blotting analysis were performed to quantify the expression of genes and proteins implicated in endoplasmic reticulum stress (ERS)-mediated apoptotic pathway. These encouraging results demonstrate that NVPS holds a great potential to serve as an effective and safe antitumor agent for chemotherapy.

2. Materials and methods

2.1. Materials and reagents

3-(4,5-dimethylthiazol-2-yl)-2,5-diphenyltetrazolium bromide (MTT), dimethyl sulfoxide (DMSO), bovine serum albumin (BSA) were purchased from Sigma. Antibody against GRP78 was obtained from Cell Signalling Technology, Inc. (Beverly, USA). Antibody against CHOP was from Protech (Wuhan, China). Antibody against Caspase-8 was purchased from Bio-world (St.Louis Park, USA). Antibodies against Activated caspase-3, Caspase-9 were obtained from Beyotime Institute of Biotechnology (China). β-tubulin and GAPDH were purchased from Abmart (Shanghai, China). Secondary anti-mouse and anti-rabbit antibodies were obtained from Invitrogen. All other chemicals and regents used in this study were of analytical grades or the highest purity grades available.

2.2. Preparation of NVPS

Food & Function Accepted Manuscript

The colonies of *Nostoc Commune* Vauch. were collected from Longnan City of Gansu Province in the autumn of 2013 and identified by a specialist. The thallus of *N. Commune* Vauch. were oven-dried at 60 °C until a constant weight (100 g) and milled into a powder using a grinder. The powder was extracted with distilled water (1:50, w/v) under reflux condition for 3 h. After two cycles, the solution was filtered and concentrated to 10% of the previous volumes with a rotary evaporator under reduced pressure. The obtained solution was deproteinized by 10.6% potassium ferrocyanide (w/v) and 21.9% zinc acetate (w/v). The process was repeated three times, and followed by centrifugation. The supernatant was dialyzed for 2 days against distilled water (Mw cutoff: 3000 Da) in order to eliminate monosaccharide, ions and other small molecules. Subsequently, 3 volumes of 95% (v/v) ethanol was added to precipitate the polysaccharides. The obtained polysaccharide was further purified by dissolution and precipitation for three times at 4°C. Finally, the refined polysaccharide pellets were dissolved completely in distilled water, and then lyophilized to yield opalescent water-soluble polysaccharides (NVPS).

2.3. Structural analysis of NVPS

Analysis of monosaccharide composition was performed by GC-MS, using a Finnigan ion trap GC-MS equipped with a DB-5 MS column. Briefly, 50 mg of NVPS fine powder was hydrolysed with 50 mL 2 M trifluoroacetic acid (TFA) at 110 °C in a sealed tube for 3 h. The hydrolysate was reduced by $NaBH_4$, followed by acidification with acetic acid. Then acetic anhydride and 1-methylimidazole were added as the acetylization reagent and catalyst of derivatization reaction, respectively. The solution

Food & Function Accepted Manuscript

was extracted twice using 2 mL of CH_2Cl_2 after termination by ddH_2O. The organic phase was removed and 200 μL of CH_2Cl_2 was added. 1 μL sample was added to auto-sampler vials with inserts and analyzed by GC-MS. Total uronic acid contents were measured by m-hydroxydiphenyl method using galacturonic acid or glucuronic acid as the standard. Fourier transform infrared (FTIR) spectra studies were performed in the range of 4000–400 cm^{-1} on TENSOR 27 FTIR spectrometer (Bruker, Germany) using the standard KBr disk method. ^1H NMR analysis of NVPS (20 mg/mL) in D_2O was carried out on a Bruker AVANCE III 600 MHz spectrometer with the operating frequency of 600 MHz.

2.4. Cell culture and maintenance

Human breast cancer MCF-7 cells and colorectal cancer DLD1 cells were incubated in RPMI-1640 medium (Gibco, USA) supplemented with 10% (v/v) heat-inactivated fetal bovine serum (FBS, Gibco) and penicillin/streptomycin (100 U/mL and 100 μg/mL, respectively; Gibco/Invitrogen, USA). MCF-7 and DLD1 cells were maintained at 37 °C with 5% fully humidified CO_2 in a Thermo Scientific Forma Direct-Heat CO_2 incubator (Thermo Fisher, USA) for 36 h and 48 h, respectively. NVPS was dissolved in RPMI-1640 medium and adjusted to various concentrations with culture medium before use.

2.5. Cell viability assay

The inhibition of NVPS on the proliferation of MCF-7 and DLD1 cells was assessed *in vitro* by MTT assay. MCF-7 and DLD1 cells (8×10^3 cells/well) were seeded in 96-well culture plates and incubated overnight. After removing the medium,

Food & Function Accepted Manuscript

100 μL NVPS of different concentrations (0, 8, 17.5, 35, 70 and 100 μg/mL) in fresh RPMI-1640 medium were added to each well, and then the wells were incubated for 36 or 48 h. After treatment, the cells were incubated with 100 μL fresh medium and 20 μL MTT solution (5 mg/mL) for another 4 h. DMSO (150 μL) was added to each well to dissolve the formazan crystals, and the absorbance at 570 nm was measured with a microplate reader (Tecan Infinite F50, Switzerland).

2.6. Cell cytotoxicity of NVPS

The cytotoxicity of NVPS toward MCF-7 and DLD1 cells was measured using a trypan blue assay. Briefly, MCF-7 and DLD1 cells were seeded in a 96-well plate at a density of 2×10^4 cells/well. After 24 h incubation at 37°C with 5% CO_2, the medium was removed and replaced with NVPS solution of different concentrations (0, 8, 17.5, 35, 70 and 100 μg/mL). After another 24 h of incubation, cytotoxicity was determined.

2.7. Colony formation assay

MCF-7 and DLD1 cells were seeded into 24-well plates at 5×10^3 cells per well and allowed to attach overnight. Various concentrations of NVPS solution (0, 35, 50, 70, 100 or 0, 70, 100, 150, 200 μg/mL) were added and incubated for six days. The cells were then fixed with 6% glutaraldehyde and stained with 0.1% crystal violet. The colony formation was captured by a stereomicroscope (SZX16, Olympus, Japan).

2.8. Apoptosis analysis and mitochondrial membrane potential (MMP) assay

MCF-7 and DLD1 cells (5×10^5 cells/well) were seeded in 6-well flat-bottom plate and incubated overnight, then treated with serial NVPS solution (MCF-7: 0, 70, 150

Food & Function Accepted Manuscript

μg/mL; DLD1: 0, 100, 200 μg/mL). Apoptosis assay was performed with annexin V-FITC apoptosis detection kit (BIO-BOX ,China) following the manufacturer's instructions. Briefly, 1.5×10^5 cells were collected, washed with cold phosphate buffered saline (PBS), and resuspended in 500 μL Annexin V binding buffer containing 5 μL Annexin V-FITC and 5 μL PI, incubated for 15 min in the dark. Flow cytometric analysis was carried out on Accuri C6 (BD Bio-science, USA). MMP was monitored using JC-1 mitochondrial membrane potential assay kit (BIO-BOX, China) according to the instruction manual. Tested cells were treated by the same procedure as above, stained with JC-1 at 37 ℃ for 20 min in darkness and analyzed for their red and green fluorescence from JC-1 using an Accuri C6 flow cytometer.

2.9. Western blotting

After NVPS treatment, cells were collected with ice-cold phosphate-buffered saline (PBS), and incubated with lysis buffer for 40 min on ice. The cell lysates were homogenized and then centrifuged at 13,000 g for 40 min at 4°C to remove cellular debris. Protein concentrations were examined by the BCA protein assay. An equal amount of protein (60 μg) were loaded in each lane, separated by 10–15% SDS-PAGE and transferred to PVDF membranes (Millipore, USA). After blocking with 5% skim milk in TBST (10 mM Tris, 150 mM NaCl and 0.1% Tween20) for 1.5 h at room temperature (RT), the membrane was incubated with primary antibodies overnight at 4°C, and subsequently with the respective horseradish peroxidase (HRP)-tagged secondary antibodies (Sigma) for 2 h at RT. The labeled proteins of interest were visualized by exposing the blots to X-ray film in a dark room using an

Food & Function Accepted Manuscript

enhanced chemiluminescence (ECL) kit (Sigma).

2.10. Quantitative real-time PCR

Total RNA was extracted from treated cells using Trizol reagent. Complementary DNA (cDNA) was synthesized from 500 ng RNA with PrimeScript RT Master Mix (Takara). All the qRT-PCR samples were performed using SYBR Green PCR Master Mix (Takara) on an Applied Biosystems Step One-Plus™ Real-Time PCR System (Applied Biosystems) under the following conditions: 95 °C for 30 s, followed by 40 cycles at 95 °C for 5 s, 64 °C for 34 s. The relative expression of each targeted gene was normalized by subtracting the corresponding GAPDH threshold cycle (Ct) values using the$\Delta\Delta$Ct comparative method. The RT-PCR primers used were as follows:

GRP78, 5′-CTGTGCAGCAGGACATCAAGTTC-3′ (forward) and
5′-TGTTTGCCCACCTCCAATATCA-3′(reverse);

CHOP, 5′-GGAAACAGAGTGGTCATTCCC-3′ (forward) and
5′-CTGCTTGAGCCGTTCATTCTC-3′(reverse);

GAPDH, 5′-GCACCGTCAAGGCTGAGAAC-3′ (forward) and
5′- TGGTGAAGACGCCAGTGGA-3′(reverse).

2.11. Statistical analysis

All determinations were performed at least three times and the data were presented as the mean ± standard deviation (SD). IC_{50} values were calculated by regression analysis. Image J software (National Institutes of Health) was used to quantify the band intensities and the Student's t-test was used to test the differences between the two groups. Differences were considered statistically significant when

Food & Function Accepted Manuscript

196 $P<0.05$.

197 ## 3. Results and discussion

198 ### 3.1. Preparation and structural characterization of NVPS

199 The procedure for preparation of the polysaccharide from *N.commune* Vauch.
200 (NVPS) is given in Fig. S1 (Supplementary data). NVPS was isolated from the thallus
201 of *N.commune* Vauch. through hot water extraction and ethanol precipitation,
202 followed by deproteinization, dialysis against water and lyophilization. The total
203 carbohydrate and uronic acid content of NVPS were 85.3% and 10.3% respectively,
204 and the extraction yield was 8.73% of dry mass. NVPS was eluted as a typical peak
205 on HPGPC, and its apparent molecular weight was estimated as 2.4×10^5 Da (data not
206 shown). The monosaccharide compositions of NVPS were determined by TFA
207 hydrolysis and GC-MS analysis, as shown in Fig. 1A and summarized in Table S1
208 (Supplementary data). It can be seen that NVPS is a representative
209 heteropolysaccharide that consists of glucose, arabinose, xylose, mannose and
210 galactose with the corresponding mole proportions of 1, 4.96, 182.02, 0.97 and 3.15,
211 respectively. Thus, xylose is the major monosaccharide constructing the backbone of
212 NVPS.

213 FTIR was used to investigate and confirm the chemical structure of NVPS. Fig.
214 1B presents the FTIR spectrum of NVPS. The large peak at around 3423 cm^{-1} is
215 assigned to the stretching vibrations of hydroxyl group. The weak absorption band at
216 about 2927 cm^{-1} was attributed to the C–H stretching vibrations.[22] The strong
217 absorption peaks at around 1630 and 1415 cm^{-1} were attributed to antisymmetric and

Food & Function Accepted Manuscript

symmetric stretching vibrations of carboxyl group, which was an indication of the presence of uronic acid in NVPS.[23] The wavenumbers between 800 and 1200 cm^{-1} represent the finger print region for carbohydrates.[24] It is noteworthy that a striking band observed at 1065 cm^{-1} is the characteristic absorption peak of furan glycosides.[25] Furthermore, the band appeared at 896 cm^{-1} is typical for β-xylans, and it is ascribed to glycosidic C_1-H deformation mode with ring vibration contribution and OH bending modes.[26–28]

In order to get more insight into the structure of NVPS, its ^1H NMR spectrum was measured in D_2O. As presented in Fig. 1C, the dominating signals at 4.404, 3.374, 3.476, 3.685, 3.998 ppm were assigned to xylose residues.[27,29,30] And the signals from other monosaccharides can not be detected, which maybe due to their much lower content when compared to xylose. This is consistent with the GC-MS results that NVPS is composed of xylose, arabinose, galactose, glucose and mannose with a ratio of 182.05:4.96:3.15:1:0.97, and xylose is the predominant component of NVPS.

3.2. Inhibition of cancer cell proliferation

To verify whether NVPS exhibits antitumor activity, we examined the effect of NVPS on proliferation of MCF-7 and DLD1 cells by MTT assays. As shown in Fig. 2A, NVPS significantly suppressed the growth of both cancer cell lines in a dose and time-dependent pattern. As summarized in Table S2 (Supplementary data), the IC_{50} values of NVPS for MCF-7 and DLD1 cell lines were 0.067 and 0.11 mg/mL respectively, indicating that NVPS has a stronger inhibitory effect against breast

Food & Function Accepted Manuscript

cancer MCF-7 cells.

In order to determine whether this inhibitory effect of NVPS on cancer cells is associated with cytotoxicity, we measured the cytotoxicity of NVPS by trypan blue colorimetric assay. It can be seen from Fig. 2B that NVPS exhibited no clear cytotoxicity against MCF-7 and DLD1 cells in a broad concentration range (8−100 μg/mL) for 24 h, the cell viability remained above 90% even at the highest concentration of 100 μg/mL. Thus the cytotoxicity of NVPS is negligible, and the anti-proliferation effect is not caused by its cytotoxicity.

To further evaluate the long-term effect of NVPS on cell survival, we performed clonogenic survival assay to examine the ability of MCF-7 and DLD1 cells to form colonies 5 days after NVPS treatment. Consistent with antiproliferative results obtained by MTT assay (Fig. 2A), a dramatic loss in colony-forming potential was observed for NVPS-treated cells as compared with controls (Fig. 2C). Colony formation of MCF-7 and DLD1 cells was reduced by approximately 50% at 50 and 70 μg/mL, respectively. On the basis of these lines of evidence, a definite conclusion can be made that NVPS exhibits a remarkable antitumor effect on MCF-7 and DLD1 cells.

3.3. Induction of apoptosis by NVPS

Cell death has conventionally been divided into three types: apoptosis, autophagy, and necrosis. Apoptosis, also known as programmed cell death, is considered to be the major type of cell death that occurs in response to most of the frontline chemotherapeutic agents. It is also a strictly regulated process of cellular suicide

Food & Function Accepted Manuscript

which is characterized by several morphological and cellular hallmarks including cell shrinkage, plasma membrane blebbing, chromatin condensation, DNA fragmentation and cleavage of key cellular proteins.[31]

To explore the underlying mechanism of cell death induced by NVPS, MCF-7 and DLD1 cells were exposed to NVPS and double stained via an FITC Annexin V Apoptosis Detection Kit followed by flow cytometry analysis. It could be seen clearly from Fig. 3A that NVPS induced apoptosis of MCF-7 and DLD1 cells in a dose-dependent manner. As presented in Fig. 3B, the fraction of Annexin V-positive MCF-7 cells was 4.5% before treatment and 17.2% and 32.1% after treatment with NVPS at concentrations of 70 and 150 μg/mL, respectively; while the fraction of Annexin V-positive DLD1 cells was 4.5% before treatment and 26.7% and 28.5% after NVPS treatment at concentrations of 100 and 200 μg/mL, respectively. Furthermore, NVPS induced higher apoptosis in MCF-7 cells (32.1%) than in DLD1 cells (28.5%) even at a lower concentration (150 vs 200 μg/mL), this was consistent with the *in vitro* MTT antitumor study (Table S2, Supplementary data). It seems that MCF-7 cells are more sensitive to NVPS than DLD1 cells. These results indicate that apoptosis induction account for the growth inhibition of MCF-7 and DLD1 cells.

3.4. Induction of the intrinsic and extrinsic apoptosis

Cell death is of vital importance for the normal development and maturation cycle, and a homeostatic balance between the rates of cell proliferation and cell death is crucial for maintaining normal physiological processes.[32] When misregulated, the apoptosis process is generally triggered, leading to various diseases including cancer.

Food & Function Accepted Manuscript

There are two classical apoptosis signaling pathways: intrinsic (mitochondrial-dependent) pathway and extrinsic (death receptor-mediated) pathway, which are characterized by cleavage activation of procaspase-9 and procaspase-8, respectively.[33,34]

The intrinsic pathway can be triggered by diverse stimuli, such as radiation, free radicals, viral infections and chemotherapeutical agents,[35] and always results in the collapse of mitochondrial membrane potential. The loss of mitochondrial membrane potential (MMP), which reflects changes in mitochondrial membrane permeability, is considered as an initial and irreversible step towards early apoptosis via intrinsic pathway.[31] The disruption of MMP led to the replacement of red fluorescence from JC-1 aggregates by green monomers. Therefore, the changes of MMP in MCF-7 and DLD1 cells after NVPS treatment were measured by JC-1 staining and flow cytometry analysis. As presented in Fig. 4A, the distribution of NVPS-treated cells shifted from the red fluorescence region (high MMP) to the green fluorescence region (low MMP). The relative fluorescent intensity ratio of red and green was shown in Fig. 4B, and NVPS induced mitochondrial membrane depolarization in a dose-dependent manner.

Moreover, the change of MMP is tightly regulated by the Bcl-2 family members that consist of pro- and anti-apoptotic proteins.[36] And there are mounting evidences that the ratio of Bax and Bcl-2, but not Bcl-2 alone, serves as a decisive player, especially during the occurrence of drug-induced apoptosis.[37] Our results from western blotting obviously disclosed that NVPS treatment elevated pro-apoptotic Bax

Food & Function Accepted Manuscript

306 while down-regulated anti-apoptotic Bcl-2 expression (Fig. 4C). A significant
307 dose-dependent increase of the Bax/Bcl-2 ratio was observed after NVPS treatment
308 (Fig. 4D). Specifically, the ratio of Bax/Bcl-2 in MCF-7 cells increased by 2.96 and
309 11.56-fold ($P < 0.01$) respectively as compared to control after exposing to NVPS at
310 concentrations of 70 and 150 μg/mL; while the ratio of Bax/Bcl-2 in DLD1 cells
311 increased by 2.28 and 5.12-fold ($P < 0.01$) respectively relative to untreated cells after
312 NVPS treatment at concentrations of 100 and 200 μg/mL. The increased Bax/Bcl-2
313 ratio is crucial for the activation of the intrinsic apoptosis pathway, and at least
314 partially responsible for the MMP loss induced by NVPS.

315 Tumor suppressor gene *p53*, which encompasses *wild type (wt)* and mutation or
316 deficiency type, plays an essential role in the regulation of cell apoptosis. However,
317 the *wt p53* is a pro-apoptotic gene in certain tumor cells such as MCF-7, while the
318 mutation *p53* is an anti-apoptotic gene in some other tumor cells such as DLD1.[38] The
319 expression of p53 leads to the downregulation of anti-apoptotic factor Bcl-2 and
320 upregulation of pro-apoptotic factor Bax.[39,40] Thus the expression of p53 protein was
321 assessed by western blotting. It could be seen from Fig. 4C that the expression level of
322 p53 increased in MCF-7 cells and decreased in DLD1 cells dramatically both in a
323 dose-dependent manner, suggesting p53 was involved in the regulation of apoptosis
324 induced by NVPS.

325 Mitochondrial membrane permeabilization results in the release of various
326 pro-apoptotic proteins such as cytochrome *c* (cyto *c*), which binds to apoptotic
327 protease-activating factor 1 (Apaf-1) and forms apoptosome. Then the initiator

Food & Function Accepted Manuscript

328 procaspase-9 is recruited and cleaved to active caspase-9, which in turn triggers the
329 activation of executioner caspase-3, leading to a cascade of caspase-mediated
330 cleavage reactions and causing cell apoptosis. Additionally, death receptor-mediated
331 extrinsic pathway requires the interaction between death receptors (such as FasR,
332 TRAIL,TNFα) on the surface of cell membranes and their respective ligands.[41]
333 Activation of these receptors typically results in the cleavage of procaspase-8, and
334 followed by the activation of downstream effector caspase-3.

335 To further examine the involvement of proteolytic caspases in NVPS-induced
336 apoptosis, the expression of caspase-9, caspase-8 and caspase-3 was determined. As
337 displayed in Fig. 4C and E, the extent of caspase-9 and caspase-8 cleavage was
338 elevated obviously and dose-dependently. In addition, the caspase-3 was further
339 activated significantly and induced apoptosis in MCF-7 and DLD1 cells after NVPS
340 treatment (Fig. 4C and E). The results indicated that NVPS could induce the apoptosis
341 in a caspase-dependent manner. All aforementioned findings reveal that the
342 anti-proliferative activity of NVPS is attributed to the activation of both extrinsic and
343 intrinsic apoptosis signaling pathways in a caspase-dependent pattern.

344 **3.5. Induction of ERS-mediated apoptosis**

345 The endoplasmic reticulum (ER) is an elaborate cellular organelle essential for
346 cell function and survival. Some perturbations in ER function can lead to the
347 accumulation of unfolded or misfolded proteins inside the ER, a cellular condition
348 commonly referred to as endoplasmic reticulum stress (ERS).[42] ERS triggers the
349 unfolded protein response (UPR), a closely orchestrated collection of intracellular

Food & Function Accepted Manuscript

signal transduction reactions designed to restore protein homeostasis. When ER stress is gradually prolonged and the protein accumulated in the ER greatly exceeds its fold capacity, cellular dysfunction and apoptotic cell death often occur.[43,44] In response to ERS, the 78-kDa glucose-regulated protein (GRP78) ER chaperone, also known as immunoglobulin heavy chain binding protein (BIP), is upregulated to stabilize protein folding. GRP78 has been recognized as an indicator of ER stress. CHOP (transcriptional factor C/EBP homologous protein), which is also referred to as GADD153, plays an important role in the UPR and it has been identified as one of the most important mediators in ER stress-induced apoptosis.[42]

In order to explore whether the NVPS induced cell death is related to ERS and ERS-mediated apoptosis, we determined the expression of GRP78 and CHOP at both the protein and mRNA level by western blotting and quantitative real-time PCR (Fig. 5). It was easy to find that NVPS treatment significantly elevated the expression of GRP78 and CHOP in both MCF-7 and DLD1 cells, and there were statistically significant differences ($P < 0.01$ or 0.05) relative to control cells (Fig. 5A and B). Furthermore, qPCR analysis clearly showed that the expression of GRP78 and CHOP at mRNA level was also upregulated (Fig. 5C). Therefore, NVPS also induced the ER stress-mediated apoptosis.

4. Conclusions

In summary, we report the isolation and *in vitro* antitumor activity evaluation of a polysaccharide from *Nostoc commune* Vauch. (NVPS) with a molecular weight about 2.4×10^5 Da. The total carbohydrate and uronic acid content of NVPS were 85.3% and

Food & Function Accepted Manuscript

372 10.3%, respectively. NVPS displayed a dose and time-dependent inhibitory effect on
373 the proliferation of MCF-7 and DLD1 cells via initiating cell apoptosis, with an IC_{50}
374 of 67 and 110 μg/mL respectively. Meanwhile, NVPS triggered the intrinsic apoptotic
375 signaling pathway, as indicated by a loss of mitochondrial membrane potential (MMP)
376 and an increase in Bax/Bcl-2 ratio. Western blotting assay showed that NVPS could
377 activate caspase-9 and caspase-8, leading to the activation of downstream effector
378 caspase-3. Intriguingly, an enhancement of Bip and CHOP expression at both protein
379 and gene level was observed after NVPS exposure, indicating that endoplasmic
380 reticulum stress (ERS)-mediated apoptotic pathway also contributes to cell apoptosis
381 in response to NVPS. The possible mechanisms involved in the activation of apoptotic
382 signaling pathway in cancer cells by NVPS were illustrated in Fig. 6. The findings of
383 this study will be helpful not only to uncover the antitumor mechanism of
384 polysaccharides from natural resources, but also to the development of effective and
385 safe polysaccharide-based antitumor agents for chemotherapy.

386 ## Acknowledgments

387 This study was supported by the National Natural Science Foundation of China
388 (nos. 31271516 and 31201072), Science Foundation for Youths of Shanxi Province
389 (2013021014-1), The R&D Infrastructure and Facility Development Program of
390 Shanxi Province (2015091015), Science Foundation of Zhejiang province
391 (LY15H280008).

392

Food & Function Accepted Manuscript

References

1. R. K. Singh, S. P. Tiwari, A. K. Rai and T. M. Mohapatra, *J. Antibiot.*, 2011, **64**, 401–412.
2. D. H. Li and Y. D. Liu, *Acta Hydrobiol. Sin.*, 2003, **4**, 408–412.
3. L. P. Brüll, Z. B. Huang, J. E. Thomas-Oates, B. S. Paulsen, E. H. Cohen and T. E. Michaelsen, *J. Phycol.*, 2000, **36**, 871–881.
4. B. Shirkey, D. P. Kovarcik, D. J. Wright, G. Wilmoth, T. F. Prickett, R. F. Helm, E. M. Gregory and M. Potts, *J. Bacteriol.*, 2000, **182**, 189–197.
5. Potts, M. *Science*, 1992, **256**, 1690–1692.
6. M. P. Briones-Nagata, M. R. Martinez-Goss and K. Hori, *J. Appl. Phycol.*, 2007, **19**, 675–683.
7. G. L. Yan, L. L. Ji, M. H. Han and D. Chen, *Acta Nutr. Sin.*, 2010, **32**, 97–98.
8. R. B. Dixit and M. R. Suseela, *Antonie van Leeuwenhoek*, 2013, **103**, 947–961.
9. S. J. Guo, S. H. Shan, X. T. Jin, Z. W. Li, Z. Y. Li, L. Q. Zhao, Q. An and W. Zhang, *J. Agric. Food Chem.*, 2015, **63**, 150–159.
10. B. Jaki, J. Orjala and O. Sticher, *J. Nat. Prod.*, 1999, **62**, 502–503.
11. B. Jaki, J. Orjala and J. Heilmann, *J. Nat. Prod.*, 2000, **63**, 1283–1285.
12. M. Ninomiya, H. Satoh, Y. Yamaguchi, T. H. akenaka and M. Koketsu, *Biosci., Biotechnol., Biochem.*, 2011, **75**, 2175–2177.
13. Y. Diao and Z. J. Yang, *Biotechnol. Bull.* 2013, **12**, 68–72.
14. G. B. Ding, H. Y. Liu, Y. Y. Lv, X. F. Liu, Y. Guo, C. K. Sun and L. Xu, *Chem. Eur. J.*, 2012, **18**, 14037–14046.

Food & Function Accepted Manuscript

15. G. B. Ding, Y. Wang, Y. Guo and L. Xu, *ACS Appl. Mater. Interfaces*, 2014, **6**, 16643−16652.

16. L. Ren, C. Perera and Y. Hemar, *Food Funct.*, 2012, **3**, 1118–1130.

17. L. Wang, Z. K. Nie, Q. Zhou, J. L. Zhang, J. J. Yin, W. Xu, Y. Qiu, Y. L. Ming and S. Liang, *Food Funct.*, 2014, **5**, 2183–2193.

18. G. B. Ding, R. H. Nie, L. H. Lv, G. Q. Wei and L. Q. Zhao, *Carbohydr. Polym.*, 2014, **109**, 28–34.

19. J. Tang and Z. Y. Hu, *Food Res. Dev.*, 2013, **9**, 1–4.

20. T. W. Zhang, L. Yang, Q. H. Liu, Q. L. Wang, Z. L. Xie and T. C. Li, *J. Food Sci. Biotechnol.*, 2011, **11**, 868–873.

21. Y. Diao, H. B. Han, Y. Li, J. P. Zhou and Z. J. Yang, *IPCBEE*, 2013, **51**, 59–63.

22. X. Xie, J. Wang and H. Zhang, *Carbohydr. Polym.*, 2015, **129**, 55–61.

23. P. Gullón, M. J. González-Muñoz, M. P. van Gool, H. A. Schols, J. Hirsch, A. Ebringerová and J. C. Parajó, *J. Agric. Food Chem.*, 2010, **58**, 3632–3641.

24. S. W. Cui, G. O. Phillips, B. Blackwell and J. Nikiforuk, *Food Hydrocolloids*, 2007, **21**, 347–352.

25. S. Li, D. Zhang, J. Wu, X. Li, J. Zhang, M. Wan and X. Lai, *Int. J. Biol. Macromol.*, 2015, **80**, 16–22.

26. M. Kačuráková, A. Ebringerová, J. Hirsch and Z. Hromádková, *J. Sci. Food Agric.*, 1994, **66**, 423–427.

27. Z. Hromádková, Z. Koštálová, N. Vrchotová and A. Ebringerová, *Carbohydr. Res.*, 2014, **389**, 147–153.

Food & Function Accepted Manuscript

28. Z. Košťálová, Z. Hromádková, B. S. Paulsen and A. Ebringerová, *Carbohydr. Res.*, 2014, **398**, 19–24.

29. R. Thangam, M. Sathuvan, A. Poongodi, V. Suresh, K. Pazhanichamy, S. Sivasubramanian, N. Kanipandian, N. Ganesan, R. Rengasamy, R. Thirumurugan and S. Kannan, *Carbohydr. Polym.*, 2014, **107**, 138–150.

30. H. Tian, X. Yin, Q. Zeng, L. Zhu and J. Chen, *Int. J. Biol. Macromol.*, 2015, **79**, 577–582.

31. S. Elmore, *Toxicol. Pathol.*, 2007, **35**, 495–516.

32. I R. Indran, G. Tufo, S. Pervaiz and C. Brenner, *Biochim. Biophys. Acta, Bioenerg.*, 2011, **1807**, 735–745.

33. A. M. Chinnaiyan, K. O'Rourke, M. Tewari and V. M. Dixit, *Cell*, 1995, **81**, 505–512.

34. M. O. Hengartner, *Nature*, 2000, **407**, 770–776.

35. P. Hensley, M. Mishra and N. Kyprianou, *Biol. Chem.*, 2013, **394**, 831–843.

36. L. A. Gillies and T. Kuwana, *J. Cell. Biochem.*, 2014, **115**, 632–640.

37. J. D. Ly, D. R. Grubb and A. Lawen, *Apoptosis*, 2003, **8**, 115–128.

38. R. Vitali, V. Cesi, B. Tanno, G. Ferrari-Amorotti, C. Dominici, B. Calabretta and G. Raschellà, *Biochem. Biophys. Res. Commun.*, 2008, **368**, 350–356.

39. J. Yu and L. Zhang, *Biochem. Biophys. Res. Commun.*, 2005, **331**, 851–858.

40. S. W. Chi, *BMB Rep.*, 2014, **47**, 167–172.

41. C. Burz, I. Berindan-Neagoe, O. Balacescu and A. Irimie, *Acta Oncol.,* 2009, **48**, 811–821.

Food & Function Accepted Manuscript

459 42. I. Tabas and D. Ron, *Nat. Cell Biol.*, 2011, **13**, 184–190.

460 43. R. Sano and J. C. Reed, *Biochim. Biophys. Acta, Mol. Cell Res.*, 2013, **1833**,

461 3460–3470.

462 44. H. Urra, E. Dufey, F. Lisbona, D. Rojas-Rivera and C. Hetz, *Biochim. Biophys.*

463 *Acta, Mol. Cell Res.*, 2013, **1833**, 3507–3517.

464

Food & Function Accepted Manuscript

Figure captions

Fig. 1. (A) (a) Typical GC chromatogram of mixed standards: (1) Rhamnitol, (2) Ribitol, (3) Fucitol, (4) Arabinitol, (5) Xylitol, (6) Mannitol, (7) Sorbitol, (8) Galactitol; **(b)** Typical GC chromatogram of NVPS.

(B) FTIR spectrum of NVPS in the range of 4000–400 cm^{-1}.

(C) ^{1}H NMR spectrum of NVPS in D_2O.

Fig. 2. *In vitro* antitumor activity of NVPS against MCF7 and DLD1 cells.

(A) Cell proliferation assay. Cells were treated with different doses (0, 8, 17.5, 35, 70 or 100 μg/mL) of NVPS for varying lengths of time (24, 36 or 48 h), and cell proliferation was measured by MTT assay.

(B) Cytotoxicity assay. Cells (2×10^4 /well) were treated with different doses for 24 h and then examined by trypan blue dye exclusion method.

(C) Dose-dependent clonogenic survival assay. Cells (5×10^3 /well) were seeded and cultured for 5 days in the absence or presence of NVPS.

Each value represents the mean ± S.D. of three independent experiments, * indicates that $P<0.05$ relative to the control cells; ** indicates that $P<0.01$ relative to the control cells.

Fig. 3. Quantitative analysis of apoptotic cells induced by NVPS.

(A) Cells were treated with NVPS for 36 h/48 h. After harvesting, cells were double-stained with Annexin V-FITC/PI and analyzed by flow cytometry. All experiments were done independently in triplicate, and representative dot plots of Annexin V-FITC/PI staining are shown. **(B)** Quantification of apoptotic cells by flow

Food & Function Accepted Manuscript

cytometry. Similar results were obtained from two other independent experiments, * $p < 0.05$ or ** $p < 0.01$ indicates statistically significant difference with untreated cells.

Fig. 4. NVPS induced intrinsic and extrinsic apoptosis in MCF7 and DLD1 cells.

(A) MCF7 and DLD1 cells were treated with different concentrations of NVPS for 36 or 48 h, stained with JC-1 dye and analyzed by flow cytometry. .

(B) Red and green fluorescence ratio of cells treated and untreated by flow cytometric analysis.

(C) Relative protein expression profile was analyzed by Western blotting. GAPDH was used as the reference control. The blots showed here are representative of three independent experiments.

(D) The corresponding ratio of Bax to Bcl-2.

(E) Densitometry analysis of relative protein expression. *$P < 0.05$ or **$P < 0.01$ compared with control.

Fig. 5. (A) Relative protein expression of ERS-induced apoptosis profile was analyzed by western blotting after treatment with different dose of NVPS for 36/48h. GAPDH was used as reference control. The blots showed here are representative of three independent experiments. The bands shown here are representative of three independent experiments.

(B) Densitometry analysis of relative protein expression.

(C) Densitometry analysis of semi-quantitative RT-PCR of ERS-induced apoptotic

Food & Function Accepted Manuscript

509 related gene expressions of cells treated with different dose of NVPS for 36/48h.
510 GAPDH gene was used as an internal loading control. The data shown represent the
511 mean ±S.D. for one experiment performed in triplicate. *P<0.05 or **P<0.01
512 relative to control.

513 **Fig. 6.** Possible schematic representations of mechanisms involved in the activation
514 of apoptotic signaling pathway in cancer cells by NVPS.

Food & Function Accepted Manuscript